International Journal of Advances in Engineering and Management (IJAEM)
Volume 3, Issue 12 Dec 2021, pp: 1434-1447 www.ijaem.net ISSN: 2395-5252

Zero Valent Iron Based Materials for the Removal of Methylene Blue

Muneeb Ahmed [*1], Muhammad Sabir Tehseen[*2], KiranFatima[*3]Alia Mushtaq[*4]

[*1]*Drugs Testing Laboratory, Rawalpindi, Pakistan*
[*2]*The University of Lahore, Sargodha Campus, Pakistan*
[*4]*University of Wah, Wah Cantt, Pakistan*
[*4]*Quaid-i-Azam University, Islamabad, Pakistan*
Corresponding Author: Muneeb Ahmed

Date of Submission: 15-12-2021 Revised: 27-12-2021 Date of Acceptance: 30-12-2021

ABSTRACT: Development of chemical methods of remediation of environmental pollutants is a well-known research area. Chemists and environmentalists are continuously involved in developing methods which can be used to deal with various environmental threats e.g., persistent organic pollutants (POPs) inorganic pollutants such as heavy metal ions etc. One of the latest terms being used is "emerging pollutants" (EPs) are defined as compounds that contaminate the environment. After 1940s, this term is frequently used by the researchers. This group of pollutants includes endocrine disrupting compounds, personal care products and pharmaceuticals. In current research work we are interested in zero valent iron (ZVI) based materials, which can be employed for the removal of emerging pollutants. Effect of the interactions between the ZVI and emerging pollutants can be studied by the modification of ZVI.

KEYWORDS: Zero Valent Iron (ZVI), Methylene Blue, Pollutants, EPs, Interaction

I. INTRODUCTION

Water pollution means any chemical, biological, or physical change that can affect the life on earth and change the environment of living organisms. Water pollution can cause so many deadly problems for the life on earth. i.e., for human and aquatic life as well. Deadly effect such as arsenicosis caused by arsenic, which is poisonous chemical released from industries, dysentery, polio, malaria, lead poisoning which is caused from substance lead, which is also released from industries, trachoma and so many other diseases caused by polluted water. Scientists workday and night to overcome these types of diseases. Physical, biological, and chemical methods are used to overcome pollution i.e., screening, sedimentation, activated sludge process, precipitation, and ion exchange method. There are so many treatments to treat the water and they are categories as primary, secondary and tertiary treatment.

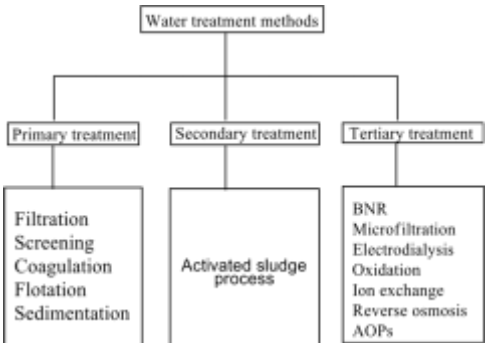

Figure 1.1: Wastewater treatment methods

1.1 Heterogenous photocatalysis

As the name indicated, there are different photocatalysts are used and these catalysts are the semiconductors. This the technique which is used for the complete degradation of the emerging contaminants from the wastewater and make it less toxic. The selection of theses semiconductors is very important for these reactions i.e., semiconductor must be nontoxic, inexpensive, and chemically stable and present in various forms. Semiconductors have valance band (VB) and conduction band (CB) which is unoccupied band. There is the band gap between the valance and

International Journal of Advances in Engineering and Management (IJAEM)
Volume 3, Issue 12 Dec 2021, pp: 1434-1447 www.ijaem.net ISSN: 2395-5252

conduction band and wide band gap which is greater than eV.

There is also required light energy when it is higher than the band gap of semiconductor there is the production of holes (h^+) and electrons (e^-) in the conduction and valance band. For the degradation of emerging pollutants there is the generation of superoxide, peroxide and hydroxyl radicals from the valance and conduction band. Mostly there is the recombination of electron/hole pair and heat generation, to avoid the recombination of electron/hole pair there is the use of semiconductors. When the hole reacts with the hydroxide ion, it produced hydroxyl radical while when molecular oxygen adsorbed on the surface reacts with the electrons it is reduced to superoxide and then react with H+ ions to produced peroxide ions.

There are so many catalysts used for the photocatalytic treatment of contaminants i.e., zero valent iron, ZnO, CdS and Fe_2O_3. TiO_2 is the most used photocatalyst which is used to treat the wastewater to make it less toxic. Catalysts are very important in their selection because they are responsible for the radical formation which is then used for treatment of water.

1.2 Zero Valent Iron

Zero valent iron (ZVI) is a reagent which is used to remediate the contaminated water. ZVI has the capacity of ground water remediation. For this purpose, any reducing agent is used for the synthesis of ZVI i.e., sodium borohydride, Green tea and eucalyptus leaf and tea polyphenol. After the synthesis, ZVI is used as an adsorbent.

There are so many reducing agents which are used to synthesize the ZVI including sodium borohydride are listed in Table 1.2.

Table 1.2: List of reducing agents

Reducing agent	**Target**
Tea polyphenol	Degradation of Bromothymol Blue
Eucalyptus leaf extracts	For treatment of eutrophic wastewater
Green tea and eucalyptus leaf	For the removal of nitrate from aqueous solutions
$NaBH_4$	Adsorption and dichlorination of trichloroethylene
Green tea leaves extract	Degradation of aqueous cationic and anionic dyes
Extract of Terminalia chebula fruit	Helps to reduce palladium and iron salts to palladium and iron NPs
Tea extracts as a catalyst for the Fentonlike oxidation of monochlorobenzene	Reduced the formation of polyphenols and caffeine which were used as a capping agent to reduce the aggregation of Fe NPs

1.3 Statement of the Problem

Literature shows that ZVI based materials are useful for elimination of EPs. However, there are some problems associated with stability of ZVI materials. It is proposed that stability of ZVI based materials can be improved using protective layers. The resulting material might be more efficient as well as stable. Our proposed coating material is silica which is mechanically and thermally stable and is a good candidate for this purpose.

1.4Objectives

1. To modify the ZVI
2. To characterize the material, we will use some analytical techniques like SEM and XRD
3. To study the interactions between ZVI and EPs will be examined by UV visible spectrophotometer.

II. EXPERIMENTATION

2.1Modification of surfactant

Ligand insertion method was used to modify the surfactant (CTAB), given by Brown and co-workers. It is cationic surfactant. For this modification equimolar ratio of halide salt of Fe and CTAB (1:1) was taken. The solvent which was used in this process is methanol and ferric chloride and CTAB was added in it. Stirred the solution for 24 hours for mixing the solution well. Then, to remove the solvent rotary evaporation was used. Sample was kept in drying oven at 60 $^{\circ}$C for the complete removal of moisture and used for proceeding work.

2.2Synthesis of FeO/SiO_2

FeO/SiO_2 was synthesized by modifying Sol gel hot injection method which is actually the method to synthesize silica partials [100]. For the synthesis of FeO/SiO_2, 0.025M Fe modified CTAB (1.22g in 100ml of distilled water) was taken and

International Journal of Advances in Engineering and Management (IJAEM)
Volume 3, Issue 12 Dec 2021, pp: 1434-1447 www.ijaem.net ISSN: 2395-5252

sonicated it until complete mixing of solution. After that, 0.0025M Na_2SiO_3 (0.305 g in 100 mL of distilled water) was taken and mix the solution well.

Gradually injected an aqueous solution of Fe modified CTAB solution into a hot Na_2SiO_3solution at 90 °C. the pH of pure Na_2SiO_3 is 14 but after adding iron solution in it the pH was 4. To maintain the pH at 9 for the better results of composite, 1M NaOH (4 g in 100 mL of distilled water) was taken in burette and added dropwise in the solution.

After that, the synthesized gel was kept cool under vigorous stirring for 30-40 minutes. After the formation of gel, the solvent was removed by vacuumed filtration. Ethanol was used for the washing of gel after filtration to reduce its oxidation. Again, washed with 20 mL distilled water.

After the filtration process, precipitates were then placed in drying oven at 90^oC to evaporate the remaining solvent in it, crystals were grinded well and annealed at 500^oC to remove the internal stress. 1 g charcoal was taken outside the crucible so that all the oxygen used for burning during annealing.

2.3Synthesis of metal

For the synthesis of metal from metal oxide, excess of sodium borohydride was taken. 1.32 g of metal oxide was dissolved in 20 mL of distilled water and added 0.33 g of sodium borohydride in the metal oxide solution. Stirred the whole solution and dried it in drying oven until all the solvent became evaporated. Grinded the crystals to fine powdered form after drying and annealed at 500^0C.

2.4Synthesis of Zero Valent Iron

Zero valent iron was synthesized by the reduction of iron (III). For the reduction of iron sodium borohydride was used in the case of iron here. For the synthesis of ZVI, iron (III) hexahydrate ($FeCl_3.6H_2O$) and sodium borohydride ($NaBH_4$) were taken. 1 g of $FeCl_3.6H_2O$ was taken and dissolved in 4/1 (v/v) methanol/water i.e., 75 mL methanol and 25 mL distilled water. Mix well and stirred on a magnetic stirrer. The solution of 0.62 g of $NaBH_4$ was prepared and poured it in a burette. Added this solution of $NaBH_4$ dropwise to the Fe (III) solution by stirring on a magnetic stirrer. Immediately black precipitates seemed after the addition of sodium borohydride solution. After the addition of sodium borohydride solution, left whole the solution for 15 minutes.

2.5Methylene blue as a targeted dye pollutant

To investigate the efficiency of photocatalytic behavior of synthesized materials, methylene blue was used as a model dye pollutant. For such purpose, stock solution of methylene blue was made and diluted it up to 50ppm solution for further use. Throughout the experiment 50ppm solution was used.

2.6Photo response of synthesized material

Using UV-Vis spectrophotometer photolysis behavior of synthesized material was observed. Various set of experiments were performed such as solution preparation and photolysis for such purpose.

2.6.1Stock solution of methylene blue

To make the 100ppm stock solution of methylene blue, take 0.1 g of methylene blue and add it in 1 liter (1000 ml) of distilled water. For further ppm solutions use the dilution formula i.e. $C_1V_1=C_2V_2$

2.6.250ppm solution of methylene blue from stock solution

A 50ppm solution was prepared by taking 100ml of methylene blue from the stock solution and add 100ml of distilled water in it and the total volume of the solution was 200ml for the photocatalysis reaction.

2.6.3Photocatalysis

A setup for photocatalysis was arranged. For this purpose, photoreactor was used. This experiment was performed by using photocatalyst. 50ppm solution was taken, added photocatalyst (20mg) (ZVI, FeO/SiO_2 and iron metal) and added hydrogen peroxide 1ml in a Patri dish. Under three conditions i.e., Dark, Visible and UV light the same solution of 50ppm was used with the total volume 200ml.

2.6.4Under dark

Under dark condition, this solution was stirred. There is no change in color. 10 readings were taken after every 10 minutes during stirring. 0.2ml sample was taken in every reading.

2.6.5Under visible light

Under visible light tungsten filament was used and same solution was taken and exposed it under the visible light. There is no change in color. Same procedure was used in this condition. After every 10 minutes 0.2ml sample was taken and total 10 samples were taken under visible condition.

2.6.6Under UV light

Same solution was taken under UV light. After every 10 minutes 0.2ml of the sample was taken. Total 10 readings were taken during stirring. The color was almost faded till the last reading. After this whole procedure, the concentration of pollutant i.e., methylene blue was determined by using UV - Visible spectrophotometer.

International Journal of Advances in Engineering and Management (IJAEM)
Volume 3, Issue 12 Dec 2021, pp: 1434-1447 www.ijaem.net ISSN: 2395-5252

III. RESULTS

3.1XRD Analysis

XRD was performed for the phase identification of synthesized material i.e., photocatalyst. Figure 3.1 shows that that XRD pattern for synthesized photocatalyst. The 2-theta value was measured in the range of 0-90 degree. Synthesized photocatalyst shows many peaks which matched with the standard with reference code 00-0020919. Comparative studies show that the synthesized photocatalyst has cubic structure. The maximum intensity showed at highest peaks present at 33.16 and 35.72 (2-theta). Other peaks are on 24.12, 40.97, 49.47, 55.33, 57.56, 62.88, 64.02, 69.73, 72.01 and 75.43 (2 theta degree). The XRD pattern showed that there is the formation of iron oxide.

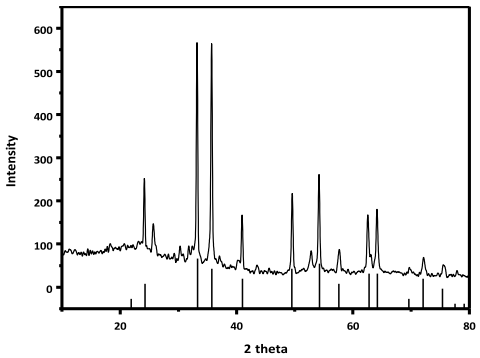

Figure 3.1: XRD pattern of iron oxide

Figure 3.2 shows that there is the formation of ZVI. The broader and intense peak matches with the standard with reference number 00-002-0919.

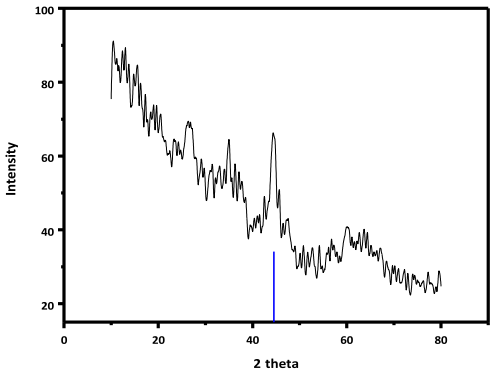

Figure 3.2: XRD pattern of ZVI

XRD spectrum shows that there is formation of SZVI. The apparent peaks on 2theta at 16.17 and 46.88 degree. Other peaks are present on 26.13 and 60.68 degree. Figure 3.3 shows the conformation of SZVI synthesis.

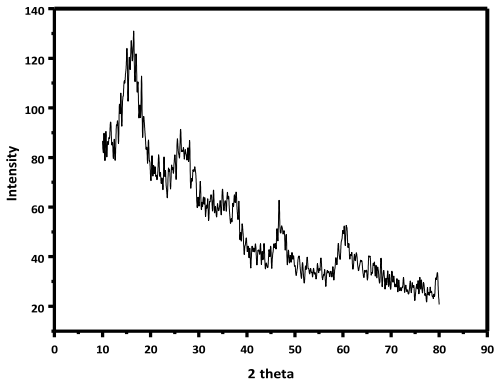

Figure 3.3: XRD pattern of SZVI

3.2SEM Analysis

SEM was performed for the examination of morphology of synthesized material. The morphology was examined with the help of scanning electron microscopy. Figure 3.4 shows that the SEM image of iron oxide synthesis and have monodisperse uniform composition.

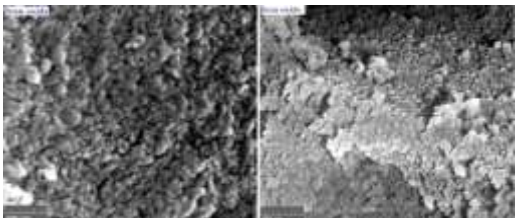

Figure 3.4: SEM images of iron oxide at 200 and 500nm resolution

In figure 3.5 ZVI particles were clearly seen. These particles having porous structure with 200 and 500 nm resolution.

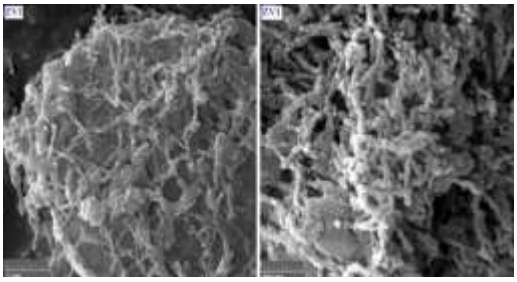

Figure 3.5: SEM images of iron oxide at 1 micrometer and 500nm resolution

International Journal of Advances in Engineering and Management (IJAEM)
Volume 3, Issue 12 Dec 2021, pp: 1434-1447 www.ijaem.net ISSN: 2395-5252

SEM images of SZVI shows that particles are porous in nature as shown in figure 3.6 on different resolutions.

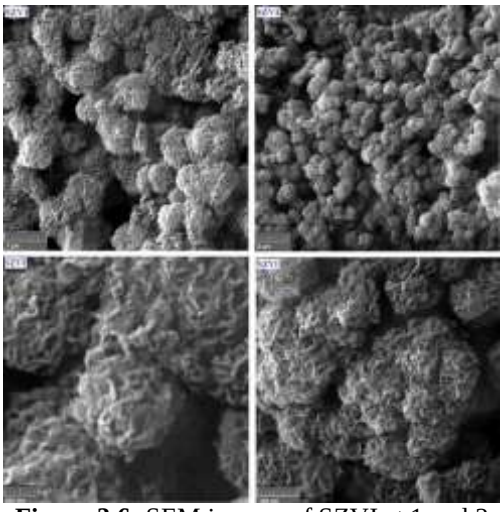

Figure 3.6: SEM images of SZVI at 1 and 2 micrometer, 200 and 500nm resolution

3.3UV-Visible Spectroscopic analysis

3.3.1UV-Visible spectrum of methylene blue

50 ppm solution of methylene blue was prepared. Further dilutions were prepared to find the λ_{max} of methylene blue solution. With the help of UV-Vis spectrophotometer, solution was scanned to find the maximum value of absorbance of MB. At 665 nm MB shows highest absorbance value as shown in figure 3.7.

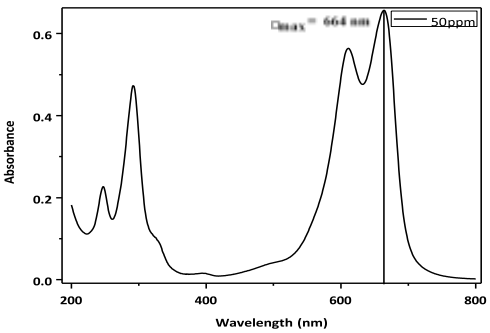

Figure 3.7: UV-Visible spectrum of MB at λmax 664 nm

3.3.2Calibration curve of Methylene Blue (MB)

From 100 ppm stock solution, different ppm solutions (50, 40, 30, 20, 10 and 5ppm) were made for the validation of lambert beer's law. By using the following dilution formula

$C_1V_1 = C_2V_2$

Spectrum was taken by using UV-Vis spectrophotometer. Set a calibration curve and It gives the slope and showing the trend of absorption following Beer Lambert's Law. Most diluted solution shows lowest absorbance. Theλ_{max} of MB was recorded at wavelength of 664nm. By UV-Vis spectrophotometer, absorbance was determined between the range of 200-800nm. From the positive value of R^2 it can be concluded that with the increase of MB concentration the absorbance become increased. It shows linearity up to 50ppm solution according to figure 3.8.

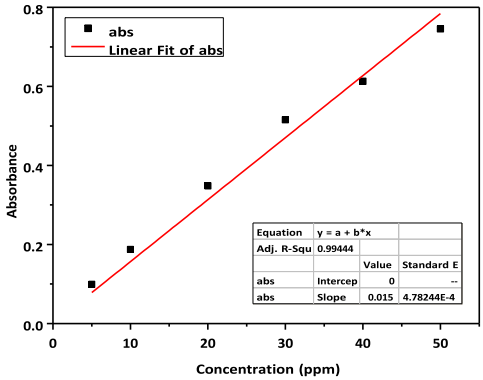

Figure 3.8: Calibration curve of MB at 664 nm

3.3.3Photo degradation of MB under different conditions

Degradation experiment was performed under different conditions i.e., under dark, visible light and UV light. These conditions were used to find out the degradation of MB that how much degradation is achieved in all three conditions.

3.3.3.1Under dark condition

The degradation experiment under dark condition was performed for 100 minutes with 10 minutes interval for each reading. UV-Vis spectrum was taken which shows was no degradation under dark condition.as shown in figure 3.9.

International Journal of Advances in Engineering and Management (IJAEM)
Volume 3, Issue 12 Dec 2021, pp: 1434-1447 www.ijaem.net ISSN: 2395-5252

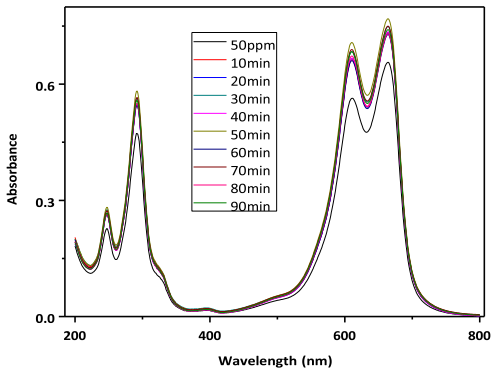

Figure 3.9: Degradation spectrum of MB under dark condition with time interval of 10 minutes

3.3.3.2% Degradation of MB

With the help of absorbance values, % degradation was calculated. It shows that there was no degradation under dark condition. So, the net degradation of MB under dark condition was 0% according to the figure 3.10.

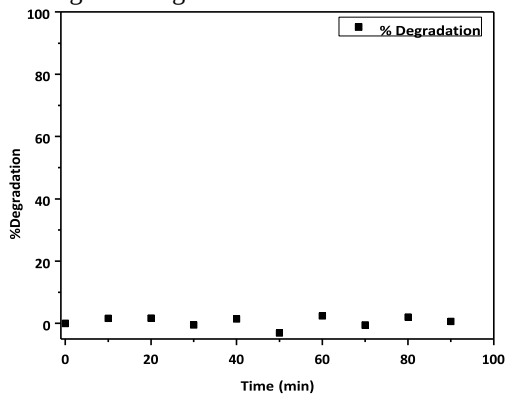

Figure 3.10: Degradation plot of MB under dark condition

3.3.3.3Under visible condition

The experiment duration for visible light degradation of MB was 90 minutes with the same interval of 10 minutes for every reading. When MB was exposed to visible light the degradation was recorded from UV-Vis spectrum which was taken for each reading.

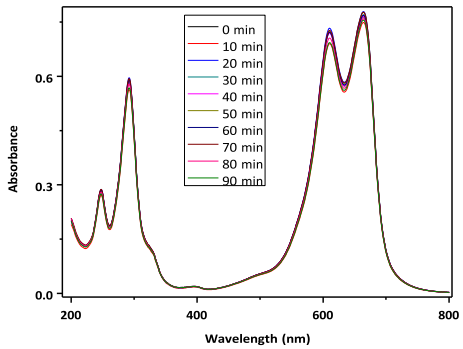

Figure 3.11: Degradation spectrum of MB under visible condition with time interval of 10 minutes

3.3.3.4Degradation of MB

From the absorbance values the degradation was recorded. After 10 minutes the degradation was maximum which is 2% as shown in figure 3.12. After that the decreased in MB degradation was observed.

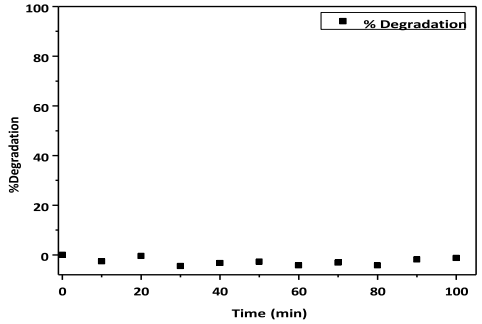

Figure 3.12: Degradation plot of MB under visible condition

3.3.3.5Under UV lamp

Within 90 minutes the experiment was completed under UV light. When MB was exposed to UV light the minute degradation was observed which is shown by the spectrum taken from UV-Vis spectrophotometer in figure 3.13.

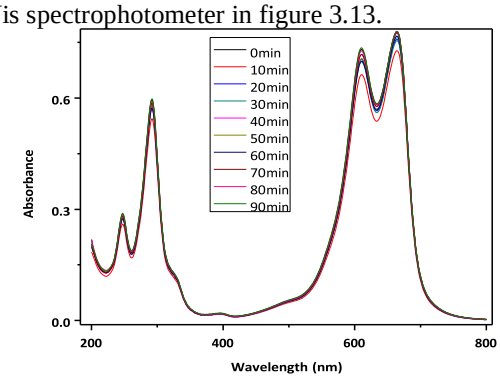

Figure 3.13: Degradation spectrum of MB under UV lamp with time interval of 10 minutes

International Journal of Advances in Engineering and Management (IJAEM)
Volume 3, Issue 12 Dec 2021, pp: 1434-1447 www.ijaem.net ISSN: 2395-5252

3.3.3.6Degradation of MB

MB was degraded when it is exposed to UV light 6% degradation was recorded after 10 minutes. After that the decreased in degradation was noted which is shown in figure 3.14.

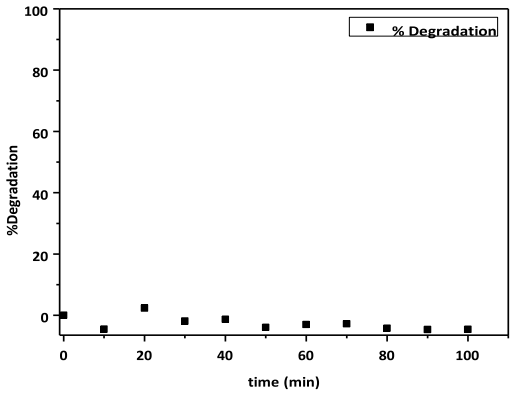

Figure 3.14: Degradation plot of MB under UV

Under dark, visible and UV condition the % degradation of 50ppm solution of MB was recorded at wavelength of 664 nm. The degradation under dark was more as compare to visible and UV region. Under dark condition the maximum degradation was recorded.

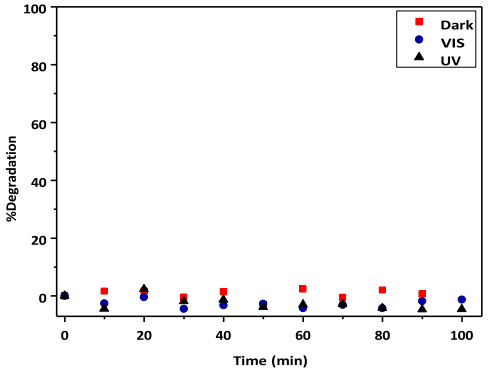

Figure 3.15: comparison of % Degradation plot of MB under different conditions

3.3.4Effect of Metal Oxide on MB degradation

3.3.4.1Under dark condition

When there is no light, UV- Vis spectra show that the absorbance was kept under wavelength of 664nm in figure 3.16. There is not huge change in the visibility of spectra.

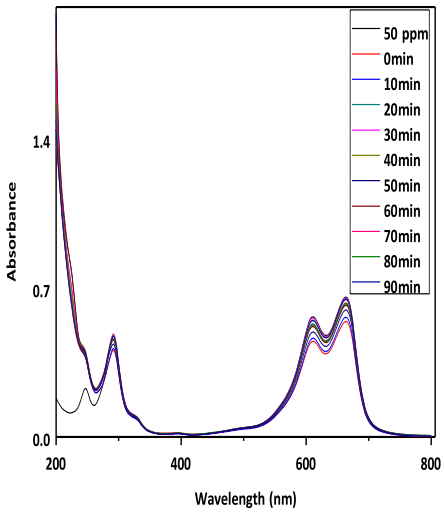

Figure 3.16: Degradation spectrum of MB with MO under dark condition with time interval of 10 minutes

3.3.4.2Effect of MO on % degradation of MB

In case of metal oxide, the absorbance value was low immediately after the addition of ZVI and H_2O_2 at 0 minute. After that there was increase in absorbance so that the removal decreases from 27% to 12 %. The removal rate was very fast at 0 minute as shown in figure 3.17.

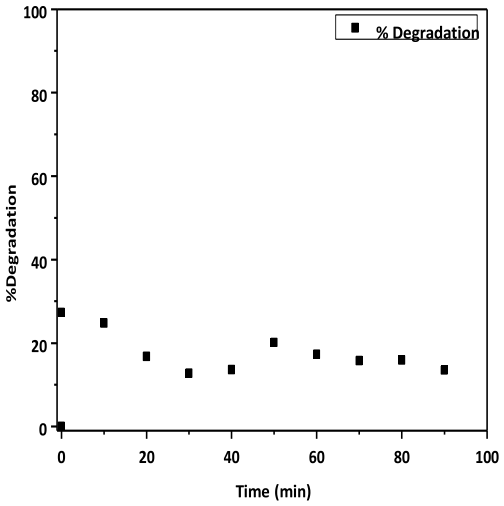

Figure 3.17: Degradation plot of MB with MO under dark condition

3.3.4.3Under visible condition

The spectra of MO show that the absorbance is maximum at 664 nm. Where the concentration of MO was low as compare to the concentration at zero minute.

International Journal of Advances in Engineering and Management (IJAEM)
Volume 3, Issue 12 Dec 2021, pp: 1434-1447 www.ijaem.net ISSN: 2395-5252

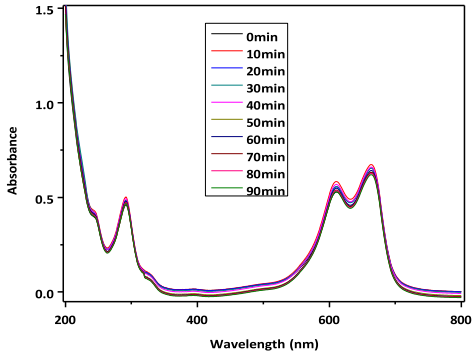

Figure 3.18: Degradation spectrum of MB with MO under visible condition with time interval of 10 minutes

3.3.4.4Effect of MO on % degradation of MB

when visible light was applied to the solution the degradation rate increased as the time increased as shown in figure 3.19. Degradation is due to the production of hydroxyl radicals. More hydroxyl radical production causes more degradation.

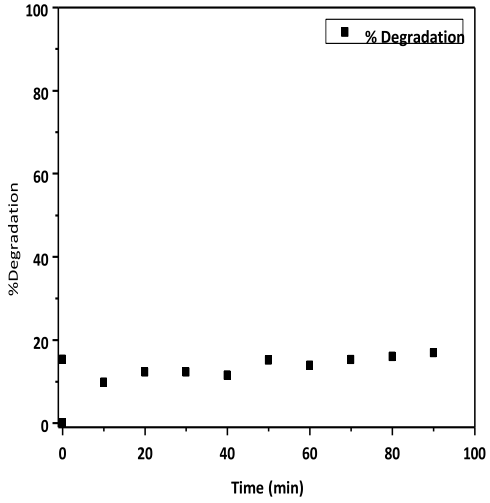

Figure 3.19: % Degradation plot of MB with MO under visible light

3.3.4.5Under UV lamp

When solution was exposed to UV light the rate of degradation became fast. The absorbance of MO was shown in figure 3.20 in the presence of UV light at different time intervals.

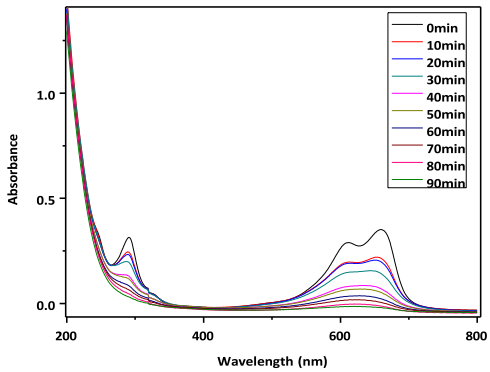

Figure 3.20: Degradation spectrum of MB with MO under UV lamp with time interval of 10 minutes

3.3.4.6Effect of MO on percent degradation of MB

It is clearly shown in figure 3.21 that the absorbance at zero minute was high so that the degradation rate was slow as compare to 100 minutes. At 0 minute the concentration of MB was maximum so that the degradation was slow as compare to 70 minutes because at 70 minutes the concentration of MB nearly approaching to zero.

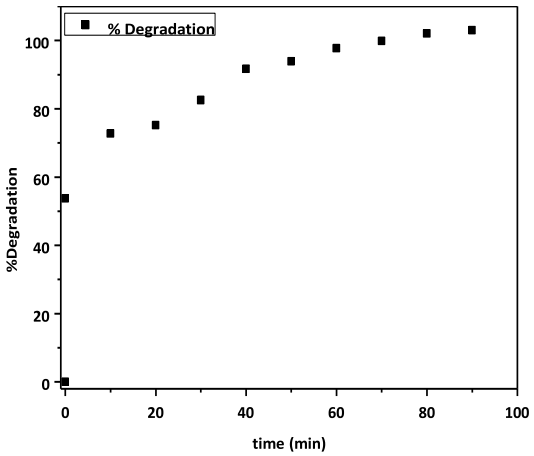

Figure 3.21: % Degradation plot of MB with MO under UV lamp

3.3.4.7Comparison of MO effect on % degradation under different conditions

Under dark condition the maximum degradation was 27% on the addition of ZVI and hydrogen peroxide at 0 minute while under visible condition the maximum degradation was 16% at 90 minutes.as shown in figure 3.22 Under UV lamp the maximum degradation was 102% at 90 minutes.

International Journal of Advances in Engineering and Management (IJAEM)
Volume 3, Issue 12 Dec 2021, pp: 1434-1447 www.ijaem.net ISSN: 2395-5252

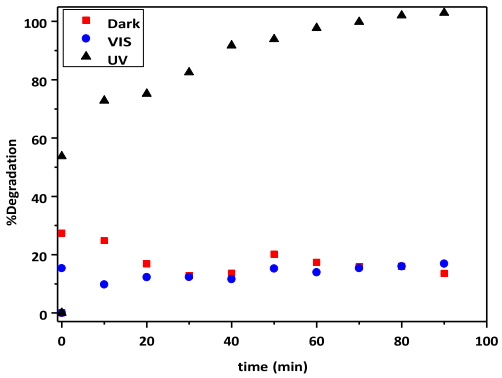

Figure 3.22: Comparison of % degradation plot of MB with MO under different conditions

3.3.5Effect of ZVI on MB degradation

3.3.5.1Under dark

The degradation pattern of MB due to ZVI and hydrogen peroxide was shown in spectra at different interval of time. Under dark condition the absorbance maxima were kept under the wavelength of 664nm.

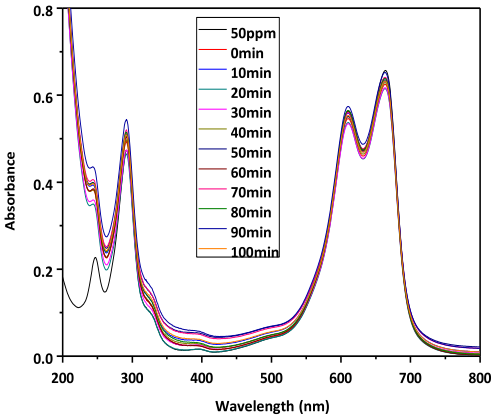

Figure 3.23: Degradation spectrum of MB with ZVI under dark condition with time interval of 10 minutes

3.3.5.2Effect of ZVI on % degradation of MB

It is clearly shown in figure 3.24 that at 0 minute the degradation rate was slow. With the passage of time the concentration of MB was decreased in the presence of ZVI and hydrogen peroxide. At 20 minutes the degradation of MB was maximum under dark condition. After that there was decreased in degradation rate.The degradation rate increased due to the production of hydroxyl radicals.

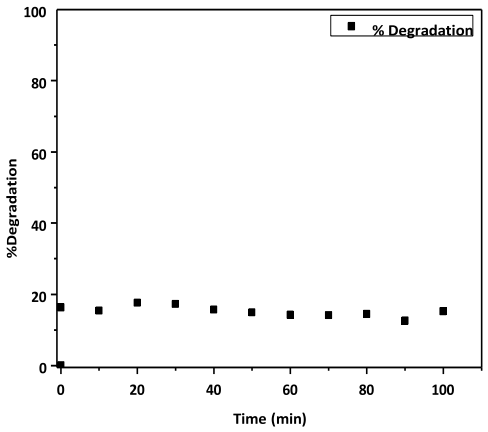

Figure 3.24: Degradation plot of MB with ZVI under dark condition

3.3.5.3Under visible light

When solution was kept under visible light, the UV-Vis spectra shows that the degradation pattern of MB in the presence of ZVI and hydrogen peroxide with the passage of time with 10 minutes difference. The absorbance was kept under visible light at 664 nm.

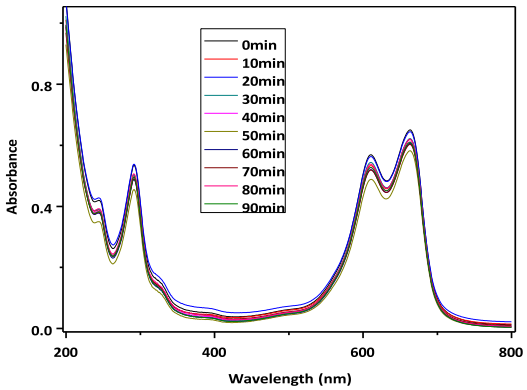

Figure 3.25: Degradation spectrum of MB with ZVI under visible light with time interval of 10 minutes

3.3.5.4Effect of ZVI on degradation of MB

With the addition of ZVI and hydrogen peroxide the degradation of MB was increased and the concentration of MB was decreased with the passage of time according to figure 3.26. It is noted that maximum degradation was 22 % after 50 minutes. At 50 minutes the degradation is maximum after that there was increased in absorbance.

International Journal of Advances in Engineering and Management (IJAEM)
Volume 3, Issue 12 Dec 2021, pp: 1434-1447 www.ijaem.net ISSN: 2395-5252

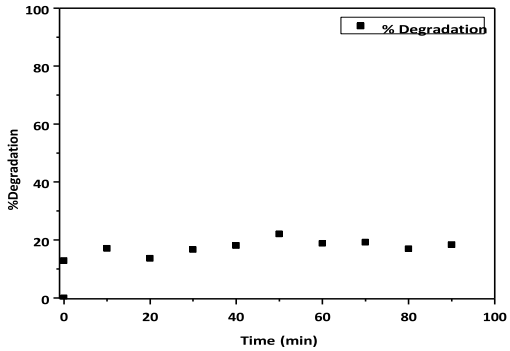

Figure 3.26: % Degradation plot of MB with ZVI under visible light

3.3.5.5Under UV light

It is clearly seen in spectra that the absorbance was minimum under wavelength of 664 nm. There was continuous decreased in absorbance at 664nm under different time intervals. The decreased in absorbance is due to the decreased in concentration of MB.

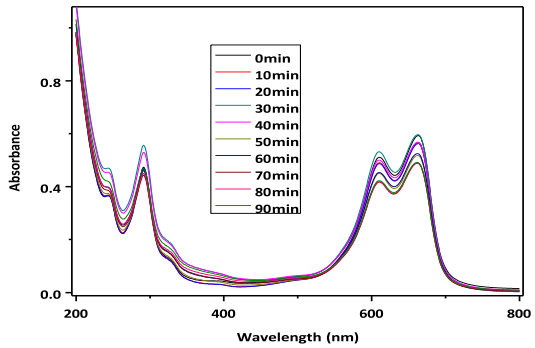

Figure 3.27: Degradation spectrum of MB with ZVI under UV light with time interval of 10 minutes

3.3.5.6Effect of ZVI on percent degradation of MB

There was continuous increased in degradation pattern as shown in figure 3.28 At zero minute the degradation was minimum but with the passage of time the degradation was maximum at 80 minutes. The maximum degradation kept under UV light at 80 minutes was 34%.

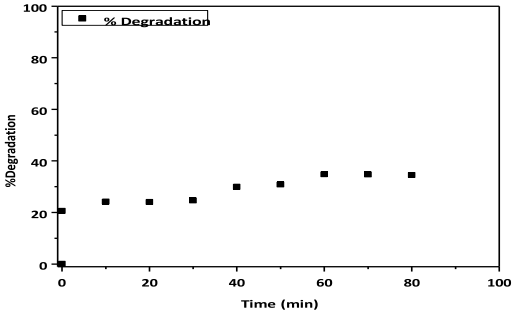

Figure 3.28: % Degradation plot of MB with ZVI under UV light

3.4.5.7Comparison of effect of ZVI on MB degradation under different conditions

Under dark condition the degradation was 17% at 30 minutes while under visible condition the removal was 22 % in 50 minutes. Under UV lamp the degradation was 34 % in 80 minutes. The degradation was increased in manner of dark, visible and UV. Degradation under visible was maximum than dark. Under UV the removal was maximum as compare to both dark and visible condition as shown in figure 3.29.

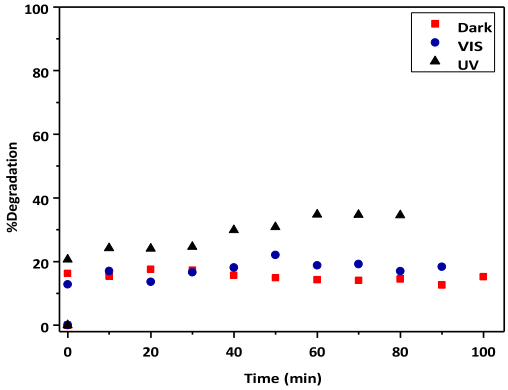

Figure 3.29: Comparison of % degradation plot of MB with ZVI under different conditions

3.3.6Effect of SZVI on MB degradation under different conditions

3.3.6.1Under dark

Under dark condition the absorbance pattern was continuously decreased with the addition of SZVI and hydrogen peroxide at different intervals of time. With the difference of 10 minutes the absorbance pattern was shown in figure 3.30at wavelength of 664nm.

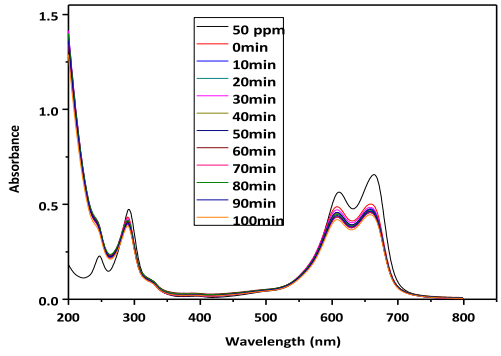

Figure 3.30: Degradation spectrum of MB with SZVI under dark condition with time interval of 10 minutes

International Journal of Advances in Engineering and Management (IJAEM)
Volume 3, Issue 12 Dec 2021, pp: 1434-1447 www.ijaem.net ISSN: 2395-5252

3.3.6.2Effect of SZVI on degradation of MB

The degradation rate was fast in the presence of catalysts. After the addition of catalysts, the degradation of MB was increased due to the hydroxyl radical production. At 0 minutes the concentration of MB is high so that the absorbance value was also maximum and degradation rate minimum as shown in figure 3.31. But after the addition of catalysts at 0 minute the degradation rate was increased immediately 34% so that the reaction rate was very fast. At 100 minute the absorbance value was minimum as compare to 0 minute and the degradation was 41 % after 100 minutes.

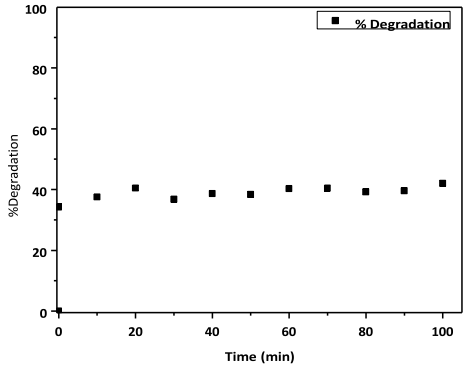

Figure 3.31: % Degradation plot of MB with SZVI under dark condition

3.3.6.3Under visible light

When the solution was exposed to visible light the absorbance of MB was decreases gradually at wavelength of 664nm with the passage of time at 10 minutes difference. The absorption pattern was shown in figure 3.32 at 664nm with the addition of SZVI and hydrogen per oxide.

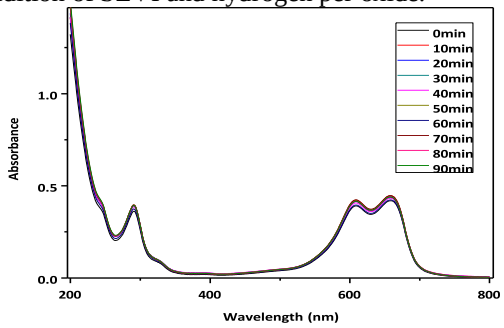

Figure 3.32: Degradation spectrum of MB with SZVI under visible condition with time interval of 10 minutes

3.3.6.4Effect of SZVI on % degradation of MB

Under visible condition the degradation rate was fast at 0 minute, but it is also noted that there is no huge difference of degradation between 0 to 90 minutes as shown in figure 3.36 At 0 minutes after addition of SZVI and hydrogen peroxide the degradation was 44 %.

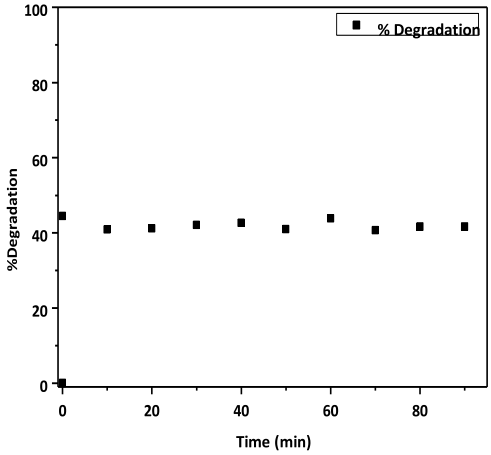

Figure 3.33: % Degradation plot of MB with SZVI under visible condition

3.3.6.5Under UV lamp

According to figure 3.34 as shown, the peak shifted from 664nm to 654 nm under UV light. The maximum absorption of MB was recorded at 664nm wavelength.

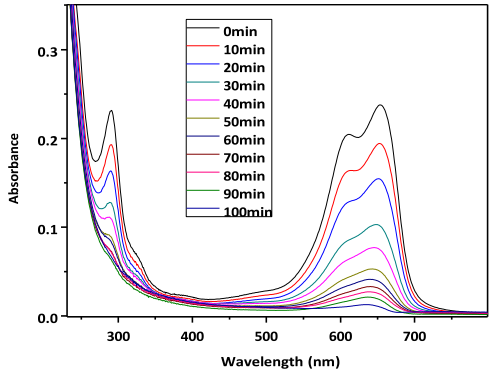

Figure 3.34: Degradation spectrum of MB with SZVI under UV condition with time interval of 10 minutes

3.3.6.6Effect of SZVI on percent degradation of MB

With the passage of time the degradation of MB was increased in the presence of catalysts under UV light as shown in figure 3.35 The concentration of Mb was higher at 0 minute as compare to 90 minutes so that the absorbance at 0 minute was minimum as compare to 100 minutes. At 0 minutes the degradation was 68% and at 100 minutes the degradation was 98%.

International Journal of Advances in Engineering and Management (IJAEM)
Volume 3, Issue 12 Dec 2021, pp: 1434-1447 www.ijaem.net ISSN: 2395-5252

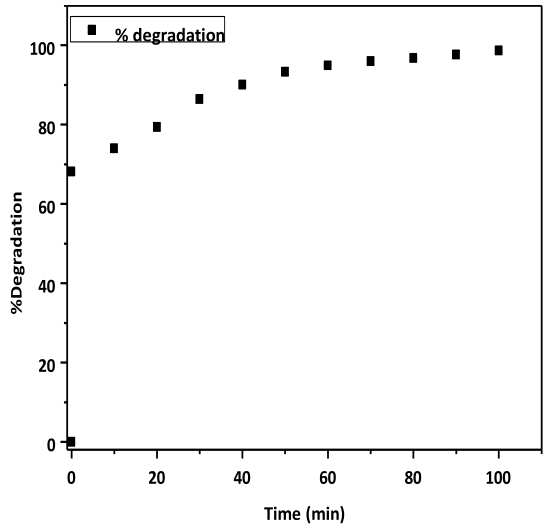

Figure 3.35: % Degradation plot of MB with SZVI under UV condition

3.4.6.7Comparison of SZVI effect on degradation of MB under different conditions

Under dark environment the degradation was 41 % in 100 minutes while under visible condition the degradation was 44 % in 0 minutes. Under UV the degradation was 98 % in 100 minutes. While comparing them, the degradation under dark was minimum while under UV degradation was maximum figure 3.36.

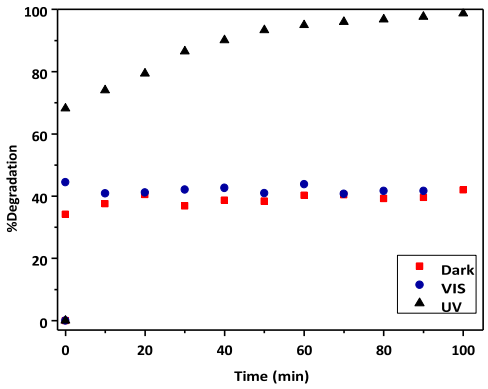

Figure 3.36: Comparison of % Degradation pattern of MB with SZVI under different conditions

IV.DISCUSSION

4.1Summary of research work

This research work was designed to synthesize SiO_2/FeO, ZVI and SZVI. To synthesize iron oxide sol gel method was used and induced metal in CTAB to increase its porosity. To check the interactions that how they interact with different dyes i.e., MB, Rh-B, MOrg and CR. UV-Vis spectrophotometer was used to check the interactions between them after every reading.

4.2XRD analysis

XRD was done for the phase identification of material which was synthesized i.e., photocatalyst. Comparative studies show that the synthesized photocatalyst has cubic structure as shown in figure 3.1. If there were no peaks found it means the synthesized material was amorphous in nature.

XRD analysis was shown in Section 3.1 for iron oxide, ZVI and SZVI from figure 3.1 to figure 3.3, the conformation of diffraction peaks was present at 2 theta which was the indication of presence of iron. In case of silica there was no peak because XRD is limited to crystalline structures only.

Figure 3.1 shows that iron oxide was synthesized. And was cubic in structure according to literature. According to figure 3.1 there was the presence of synthesized material in case of iron oxide. The most intense peaks were present on 33.29, 35.72 degree at 2theta. Other peaks are present at 24.12, 40.97, 49.60, 54.06, 57.07, 62.55, 64.04,72.13 and 75.49 degree.

In case of zero valent iron figure 3.2 shows the broad peak on 44.45 degree at 2 theta which is the indication of the presence of ZVI. According to literature the crystalline structure of ZVI was cubic.

4.3SEM analysis

In figure 3.4 the SEM result of iron oxide was shown. Particles are homogeneously arranged and are clearly shown. The particles were not agglomerated. The SEM image shows the conformation of iron oxide particles synthesis. First image shows the 200nm resolution of iron oxide in which particles are arranged in order while in 500nm resolution the particles are closely packed and arranged as well.

According to the literature, core shell structure represents ZVI with hollow spaces which indicates oxidized part of iron oxide. These shells are responsible of resistant to further oxidation.

In case of SZVI, particles are hollow in structure which represents the porosity of SZVI. The material was more porous which is responsible for the better degradation efficiency of the pollutant. It acts as pollutant removal agent against dyes. In first image with 1 micrometer resolution, it is clearly shown that particles are porous in structure but in 500 nm resolution image particles of SZVI are clearly visible.

International Journal of Advances in Engineering and Management (IJAEM)
Volume 3, Issue 12 Dec 2021, pp: 1434-1447 www.ijaem.net ISSN: 2395-5252

4.4UV VIS- spectroscopic analysis

Under different conditions different dyes behaves differently. with catalysts dyes degraded well other than without catalysts. UV light effect the catalysis process in case of degradation of dyes. In figure 4.1 the response of all the dyes under dark condition observed. There is no response towards degradation as they are responsible of adsorption assisted photocatalysis. In the figure shown only MB with SZVI response well as compare to all other dyes but it was not much better result.

CONCLUSION

- ✓ It is concluded that synthesized materials (photocatalyst) are more efficient in degradation of dyes under UV lamp.
- ✓ The degradation is fast with catalyst as compare to without catalyst. It means the rate of reaction is fast with catalysts.
- ✓ The degradation of dyes in the presence of photocatalyst is not time consuming because within less than a minute the degradation approaches to maximum degradation values.
- ✓ The synthesized material is more stable in degradation of dyes.

REFERENCES

[1]. Schwarzenbach, R.P., Egli, T., Hofstetter, T.B., Von Gunten, U. & Wehrli, B. (2010). Global water pollution and human health. Annu. Rev. Environ. Resour. 35, 109-136.

[2]. Wang, Q. & Yang, Z. (2016). Industrial water pollution, water environment treatment, and health risks in China. Environ. Pollut. 218, 358-365.

[3]. (a) Shiklomanov, I.A. (2000). Appraisal and assessment of world water resources. Water Int 25, 11-32; (b) Halacy Jr, D. (1977). Earth, water, wind, and sun: our energy alternatives.

[4]. Ma, J., Ding, Z., Wei, G., Zhao, H. & Huang, T. (2009). Sources of water pollution and evolution of water quality in the Wuwei basin of Shiyang river, Northwest China. J. Environ. Manage. 90, 1168-1177.

[5]. Myers, C.F., Meek, J., Tuller, S. & Weinberg, A. (1985). Nonpoint sources of water pollution. J Soil Water Conserv 40, 14-18.

[6]. Freeman III, A.M. (1982). Air and water pollution control: a benefit-cost assessment.

[7]. Jafarzadeh, H.N.E., Rostami, S., Sepehrfar, K. & Lahijanzadeh, A. (2004).

[8]. Identification of the water pollutant industries in Khuzestan Province.

[9]. Stein, E.D., Tiefenthaler, L.L. & Schiff, K.C. (2007). Sources, patterns and mechanisms of storm water pollutant loading from watersheds and land uses of the greater Los Angeles area, California, USA. SCCWRP 510.

[10]. Mitra, A. & Gupta, S. (1999). Effect of sewage water irrigation on essential plant nutrient and pollutant element status in a vegetable growing area around Calcutta. J.

[11]. Indian Soc. Soil Sci.

[12]. Freeman Jr, D.C. & Rogers, L.J., Analysis of organic and inorganic water pollutants. Google Patents: 1972.

[13]. Wang, Y.-S., Subba-Rao, R. & Alexander, M. (1984). Effect of substrate concentration and organic and inorganic compounds on the occurrence and rate of mineralization and cometabolism. Appl. Environ. Microbiol. 47, 1195-1200.

[14]. Martínez-Huitle, C.A., Rodrigo, M.A., Sirés, I. & Scialdone, O. (2015). Single and coupled electrochemical processes and reactors for the abatement of organic water pollutants: a critical review. Chem. Re. 115, 13362-13407.

[15]. Orubu, C.O. & Omotor, D.G. (2011). Environmental quality and economic growth: Searching for environmental Kuznets curves for air and water pollutants in Africa. Energy Policy 39, 4178-4188.

[16]. Cooper, C. (1993). Biological effects of agriculturally derived surface water pollutants on aquatic systems—a review. J. Environ. Qual. 22, 402-408.

[17]. Alvarino, T., Torregrosa, N., Omil, F., Lema, J. & Suarez, S. (2017). Assessing the feasibility of two hybrid MBR systems using PAC for removing macro and micropollutants. Journal of environmental management 203, 831-837.

[18]. Kasprzyk-Hordern, B., Dinsdale, R.M. & Guwy, A.J. (2009). Illicit drugs and pharmaceuticals in the environment–forensic applications of environmental data. Part 1: estimation of the usage of drugs in local communities. Environ. Pollut. 157, 17731777.

[19]. PPCP, C. (2003). High on pollution: drugs as environmental contaminants. J. Environ. Monit, 5.

[20]. Gardner, C. & Guy, A. (1984). A social interaction model of anxiety sensitive to

acutely administered benzodiazepines. Drug Dev. Res. 4, 207-216.
[21]. Cone, E.J. (2001). Legal, workplace, and treatment drug testing with alternate biological matrices on a global scale. Forensic Sci. Int. 121, 7-15.
[22]. Ernst, E. (2002). Adulteration of Chinese herbal medicines with synthetic drugs: a systematic review. J. Intern. Med. 252, 107-113.
[23]. Arnold, C. (2013). The new danger of synthetic drugs. Lancet 382, 15-16.
[24]. Belcaro, G. & Nicolaides, A. (2001). A new role for natural drugs in cardiovascular medicine. Angiology 52, S1.
[25]. Ma, C.-l. & Sun, X.-d. (2002). Preparation of nanocrystalline metal oxide powders with the surfactant-mediated method. Inorg. Chem. Commun 5, 751-755.
[26]. Hameed, A., Dewayanto, N., Dongyun, D. & Nordin, M. In Synthesis and Characterization of Nano Scale Zero-ValentIron Supported on Mesoporous Silica, 9th Joint Conference on Chemistry, 2014.
[27]. Su, Y., Adeleye, A.S., Huang, Y., Zhou, X., Keller, A.A. & Zhang, Y. (2016). Direct synthesis of novel and reactive sulfide-modified nano iron through nanoparticle seeding for improved cadmium-contaminated water treatment. Sci. Rep. 6, 24358.